

Published in final edited form as:

*J Immunol.* 2022 July 15; 209(2): 379–390. doi:10.4049/jimmunol.2101139.

## KIR2DS2 expression identifies NK cells with enhanced anti-cancer activity

Matthew D. Blunt<sup>#\*</sup>, Andres Vallejo Pulido<sup>#\*</sup>, Jack G. Fisher<sup>\*</sup>, Lara V. Graham<sup>\*</sup>, Amber DP. Doyle<sup>\*</sup>, Rebecca Fulton<sup>\*</sup>, Matthew J. Carter<sup>†</sup>, Marta Polak<sup>\*</sup>, Peter WM. Johnson<sup>†</sup>, Mark S. Cragg<sup>†</sup>, Francesco Forconi<sup>†</sup>, Salim I. Khakoo<sup>\*</sup>

<sup>\*</sup>School of Clinical and Experimental Sciences, University of Southampton, UK

<sup>†</sup>School of Cancer Sciences, University of Southampton, UK

<sup>#</sup> These authors contributed equally to this work.

### Abstract

Natural killer (NK) cells are promising cellular therapeutics against haematological and solid malignancies. Immunogenetic studies have identified that various activating killer cell immunoglobulin-like receptors (KIR) are associated with cancer outcomes. Specifically, KIR2DS2 has been associated with reduced incidence of relapse following transplantation in haematological malignancies and improved outcomes in solid tumours, but the mechanism remains obscure. Therefore we investigated how KIR2DS2 expression impacts NK cell function. Using a novel flow cytometry panel, we show that human NK cells with high KIR2DS2 expression have enhanced spontaneous activation against malignant B cell lines, liver cancer cell lines and primary chronic lymphocytic leukaemia (CLL) cells. Surface expression of CD16 was increased on KIR2DS2<sup>high</sup> NK cells and accordingly, KIR2DS2<sup>high</sup> NK cells had increased activation against lymphoma cells coated with the clinically relevant anti-CD20 antibodies rituximab and obinutuzumab. Bulk RNA sequencing revealed that KIR2DS2<sup>high</sup> NK cells have upregulation of NK mediated cytotoxicity, translation and FCGR gene pathways. We developed a novel single-cell RNA sequencing technique to identify KIR2DS2+ NK cells and this confirmed that KIR2DS2 is associated with enhanced NK cell mediated cytotoxicity. This study provides evidence that KIR2DS2 marks a population of NK cells primed for anti-cancer activity and indicates that KIR2DS2 is an attractive target for NK based therapeutic strategies.

### Introduction

NK cells are powerful effector cells in the anti-cancer immune response and act via direct recognition and killing of tumour cells, promotion of adaptive immune responses, and antibody-dependent cellular cytotoxicity (ADCC)(1–3). There is intense interest in targeting

Correspondence to: Matthew D. Blunt.

To whom correspondence should be addressed: Dr Matthew D. Blunt, School of Clinical and Experimental Sciences, Level E, South Academic Block, SouthamptonGeneralHospital, University of Southampton, SO16 6YD, m.d.blunt@soton.ac.uk, Tel: 023 8120 6671.

#### Conflict of Interests

MDB, RF and SIK have applied for a patent for peptide mediated NK cell activation. All other authors declare that they have no relevant conflicts of interest.

NK cells for cancer therapy via adoptive cellular therapies as well as via antibody and cytokine mediated stimulation(1, 3, 4).

NK cells are regulated by the integration of signals from an array of non-rearranged activating and inhibitory receptors, of which the killer cell immunoglobulin-like receptors (KIR) are an important component(5). Both KIR and NKG2A/C interact with HLA class I molecules and the inhibitory KIR have been well described to sense downregulation of HLA class I and generate inhibitory signals(5). In contrast, there is much less understanding of how activating KIR regulate the activity of NK cells against cancer cells. This is important because there is more population diversity in expression of activating KIR than their inhibitory counterparts, and thus in the innate genetic susceptibility to cancer(6). Difficulties in understanding the activating KIR have primarily been caused by a lack of antibodies able to sufficiently discriminate from inhibitory KIR with high sequence homology(6–8). In addition, activating KIR ligands have been hard to define(6) due to a lower affinity for HLA class I compared to inhibitory KIR(6, 9). Thus, the study of KIR2DS2 has previously been limited in part due to a lack of available antibodies able to discriminate KIR2DS2 from the closely related inhibitory KIRs KIR2DL3 and KIR2DL2. We have however recently shown that KIR2DS2 binds HLA-C in combination with viral peptides containing an alanine and threonine at the carboxy-terminal -1 and -2 of the peptide(10) and developed an antibody combination able to detect NK cells enriched for KIR2DS2 relative to KIR2DL3 and KIR2DL2(11). In addition, using a reporter cell line, KIR2DS2 has been shown to recognise a  $\beta$ 2-microglobulin independent ligand on cancer cells(12).

There is substantial diversity in the number of KIR genes that individuals have and these are encoded as two haplotypes(13). The KIR A haplotype consists of predominantly inhibitory KIR and one activating KIR (KIR2DS4), whilst the KIR B haplotype encodes a more variable gene content which includes more activating KIR (KIR2DS1, KIR2DS2, KIR2DS3, KIR2DS5 and KIR3DS1). KIR gene diversity has been implicated in anti-tumour responses in a number of genetic studies, with the KIR B haplotype associated with improved outcome in haematological malignancies following transplantation treatment(14–18). In addition, activating KIR are associated with protection against the development of childhood acute lymphoblastic leukaemia (ALL)(19), with the greatest reduction in risk by activating KIR for developing ALL conferred by KIR2DS2. Expression of KIR2DS2 on donor cells during transplantation has also been shown to significantly improve progression free survival and reduce relapse rates in patients with haematological malignancies including non-Hodgkin lymphoma(14, 20). In accordance with this, cord blood derived NK cells with a KIR2DS2-positive genotype showed increased activation against K562 targets cells in vitro as compared with KIR2DS2-negative NK cells(20). In addition, KIR2DS2 is associated with increased activation against glioblastoma cells(21) and improved clinical response in breast cancer, colorectal cancer, non-small cell lung cancer and hepatocellular carcinoma(22–25). However, these studies have been unable to discriminate between KIR2DS2 and the closely related inhibitory KIRs KIR2DL3 and KIR2DL2 because of the strong linkage disequilibrium between KIR2DS2 and KIR2DL2 in genetic studies and a lack of discriminatory antibodies in functional studies.

NK cells are also important determinants of treatment success with monoclonal antibodies. Anti-CD20 antibody therapies have revolutionised the treatment of B cell malignancies and ADCC mediated by NK cells is thought to contribute to the therapeutic response(26–28). NK cells express the Fc receptor CD16, enabling them to execute ADCC(28). KIR2DS2 positive NK cells have enhanced CD16 expression compared to KIR2DS2 negative NK cells(21), and the presence of KIR2DS2 is associated with enhanced ADCC to anti-GD<sub>2</sub> and prolonged event-free survival during anti-GD<sub>2</sub> treatment for neuroblastoma(29). Whether KIR2DS2 affects NK cell activation in response to anti-CD20 antibodies however is unknown. This is important given the beneficial role of activating KIR in patients with haematological malignancies and in the requirement for identification of highly active subsets of NK cells to improve response to immunotherapies. Here, we use our recently developed flow cytometry based discrimination technique(11) and novel single-cell RNA sequencing approach in which coupled KIR sequencing occurs, to investigate the potential basis of the enhanced activity of KIR2DS2+ NK cells against cancer targets.

## Materials and Methods

### Samples and cell lines

Healthy donor PBMC (Peripheral Blood Derived Mononuclear Cells) were obtained with full ethical approval from the National Research Ethics Committee (reference 06/Q1701/120) and cryopreserved in liquid nitrogen until use. Chronic lymphocytic leukaemia (CLL) samples were obtained from patients attending Southampton General Hospital following written informed consent and in accordance with Ethics Committee approvals (UK National Research Ethics Service number 19/WM/0262) and the Declaration of Helsinki. CLL patient PBMC were obtained and cryopreserved in liquid nitrogen until use.

Cell lines used as targets in functional assays were: Mino, DOHH2, REH, Ramos, HBL-1, SU-DHL-6, SU-DHL-4, Raji, JeKo-1, Granta-519, MAVER-1, the HLA-null transformed B lymphoblastoid cell line 721.221, SNU-398, HepG2 and PLC/PRF/5. All cell lines were cultured in RPMI 1640 medium supplemented with 1% penicillin-streptomycin (Life Technologies) and 10% heat inactivated fetal bovine serum (FBS; Sigma).

### Staining of cells for flow cytometry

Healthy PBMC or isolated NK cells (average purity of 96% NK cells achieved using the Miltenyi Biotec NK isolation kit) were blocked with 10% AB serum for 20 minutes at 4°C then washed and stained with antibodies for 30 minutes at 4°C in FACs buffer (PBS, BSA 1%, Sodium Azide 0.05%). Surface antibodies used were REA147-FITC (Miltenyi Biotec), CH-L-PE (BD Biosciences), CD56-PE/Cy7 (Biolegend) CD3-PerCP (Biolegend) and CD16-APC (Biolegend). Cells were then washed in FACs buffer and analysed by flow cytometry using a BD FACs Aria. Analysis was performed using FlowJo\_V10 software. For HLA-C staining, B-cell lines were incubated with DT9 antibody for 30 minutes in FACs buffer then washed in FACs buffer and stained with anti-mouse secondary antibody-AF647. Cells were then analysed by flow cytometry using a BD Accuri and data analysed by FlowJo\_V10.

### NK cell degranulation assay

Healthy donor PBMCs or isolated NK cells were stimulated overnight with IL-15 (1ng/ml; R&D Systems) and co-incubated with target cells at 10:1, 5:1 or 1:1 effector:target ratios as indicated for 4 hours with anti-CD107a-AF647. For assays using primary CLL cells as targets, CLL cells were isolated using a B-CLL isolation kit (Miltenyi Biotech) before co-incubation with healthy donor PBMC. For assays in combination with anti-CD20 antibodies, target cells were incubated with indicated antibody (1µg/ml; in-house) for 20 minutes at 4°C prior to addition of PBMC or purified NK cells (Miltenyi Biotech NK isolation kit) at a 10:1 effector:target ratio. Excess anti-CD20 antibody in the medium was removed by two washes with RPMI media prior to addition of PBMC. Golgistop (BD Biosciences) was added 1 hour after co-incubation and cells were then stained with REA147-FITC (Miltenyi Biotech), CH-L-PE (BD Biosciences), CD56-PE/Cy7 (Biolegend) CD3-PerCP (Biolegend) and analysed by flow cytometry on a BD FACS Aria. Data was analysed by FlowJo\_V10 software.

### Intracellular cytokine staining of human cells

Healthy donor PBMCs were stimulated overnight with IL-15 (1ng/ml) and then co-incubated with target cells at 5:1 effector:target ratio for 4 hours. Golgistop (BD Biosciences) was added 1 hour after co-incubation and cells were then stained for surface markers REA147-FITC (Miltenyi Biotech), CH-L-PE (BD Biosciences), CD56-PE/Cy7 (Biolegend) and CD3-PerCP (Biolegend). Cells were then fixed and permeabilized, stained for IFN $\gamma$ -BV421 (Biolegend) and TNF $\alpha$ -AF700 (Biolegend) and analysed by flow cytometry on a BD FACS Aria. Data was analysed by FlowJo\_V10 software.

### Bulk RNA sequencing

KIR2DS2<sup>high</sup>, KIR2DL3/L2<sup>high</sup> and KIR2DL3/L2/S2- CD56dim CD3- healthy human cells were sorted using a BD FACS Aria and the above described surface staining protocol with antibodies REA147-FITC, CH-L-PE, CD56-PE/Cy7 and CD3-PerCP. RNA was subsequently isolated using the RNeasy Kit (QIAGEN) according to the manufacturer's instructions. All samples were subjected to an indexed paired-end sequencing run of 2x150 cycles on an Illumina NovaSeq6000 at 20M reads per sample. Paired-end sequence reads were quantified to transcript abundance using Kallisto (30) with bias correction, and 50 bootstrap samples. Reads were mapped to ENSEMBL release 95. On average, the percentage of exonic aligned reads was 56.5%. The transcript abundance was then summarized to gene level using Sleuth (31).

Raw counts from RNA-sequencing were processed in the Bioconductor package EdgeR<sup>(32)</sup>, variance was estimated, and size factor normalized using Trimmed Mean of M-values (TMM). Genes with a minimum of 2 reads at a minimum of 50% samples were included in the downstream analyses. All fit models included a term to model individual variation. For the identification of differentially expressed genes (DEGs) among the 3 groups (KIR2DS2<sup>high</sup>, KIR2DL3/L2<sup>high</sup> and KIR2DL3/L2/S2-), a paired model was used in all the possible pairs. Genes with a false discovery rate (FDR)-corrected p-value < 0.05 resulting from a likelihood ratio test using a negative binomial generalized linear model fit were

identified as differentially expressed. Gene ontology and pathway enrichment analysis were done using Camera(33) and Ensemble of Gene Set Enrichment Analyses (EGSEA)(34).

### Single-cell RNA sequencing

Single cell libraries were generated using the Chromium Single Cell 3' library and gel bead kit v3.1 from 10x Genomics. Briefly, single cell suspensions were tagged using TotalSeq™ hashtag antibodies (Biolegend). After pooling, 10,000 cells were loaded onto a channel of the 10x chip to produce Gel Bead-in-Emulsions (GEMs). This underwent reverse transcription to barcode RNA before clean-up and cDNA amplification followed by enzymatic fragmentation and 5' adaptor and sample index attachment. Libraries were sequenced on the NextSeq500 (Illumina) with 28x60 bp paired-end sequencing.

### KIR Long read sequencing

KIR molecules were enriched and sequenced using a modified RAGE-seq protocol(35). Briefly, 3ng of full length cDNA from the short read experiment was amplified by PCR using KAPA HotStart HIFI ReadyMix (Kappa Biosystems) with the following cycling conditions: 98°C for 3 min; [98°C for 20 s, 65°C for 30 s, 72°C for 2 s] × 10 cycles 72°C for 3 min. After purification with AMPure beads(Beckman), samples were incubated at 65 °C to produce ssDNA and then KIR molecules captured using a pool of custom designed probes (Table 1). Washes were made following the xGen hybridization capture protocol (IDT). Captured molecules were amplified by PCR and purified using the same procedure as before. Nanopore libraries were prepared using the LSK-110 kit and sequenced on a MinION flow cell (R9.4.1).

### Bioinformatic analysis

For short read alignment, read filtering, barcode and UMI counting were performed using Cell Ranger v6.0. High quality barcodes were selected based on the overall UMI distribution using emptyDrops(36). All further analyses were run using the Python-based Scanpy(37). To remove low quality cells, we filtered cells with a high fraction of counts from mitochondrial genes (20% or more) indicating stressed or dying cells(38). In addition, genes expressed in less than 20 cells were excluded. Cell by gene count matrices of all samples were concentrated to a single matrix and values log transformed. To account for differences in sequencing depth or cell size UMI counts were normalized using variance-stabilizing transformation. The top variable genes were selected based on normalized dispersion. This output matrix was input to all further analyses except for differential expression testing where all genes were used.

For long reads, raw Nanopore data were basecalled using Guppy (v4.4.2) using Google Colab. The basecalled reads were processed for removing low quality reads and extracting reads containing barcodes and UMI sequences matching the Illumina library using Sichelore(39). QC passing reads were demultiplexed using the top barcodes from the short read data(35). Single cell individual FASTQ files were mapped against IPD-KIR Sequence database(40, 41) using minimap2 (v2.17) with the parameters “-ax map-ont -p 0 -N 10,” to keep multimapping reads. Transcript abundance was estimated using the expectation-maximization approach algorithm (Nanocount)(42). Output abundance data was compiled

and collapsed by gene name using custom python scripts and further analyzed using scanpy(37). Nanopore data was integrated to the short read data by sharing the UMAP representation coordinates.

## Statistical analysis

For experimental data, statistical analysis was performed using Graph-Pad Prism 8.0 software. Normal distribution of data was evaluated by the Shapiro-Wilk test and statistical significance was determined using student's two-tailed *t* tests, Wilcoxon signed rank test or two-way ANOVA as appropriate. Data was considered statistically significant at  $p < 0.05$ .

## Results

### KIR2DS2<sup>high</sup> NK cells have enhanced activation against malignant cells

The presence of the gene for KIR2DS2 within an individual is associated with improved clinical responses in patients with B cell malignancies(19, 20). To investigate the basis behind this association, we investigated, at a functional level, the relationship between the expression of KIR2DS2 and activation of NK cells against a number of malignant B cell lines. We used the recently described antibody combination of REA147 and CH-L to separate CD3-CD56dim NK cells based on high expression of KIR2DS2 (KIR2DS2<sup>high</sup>), high expression of KIR2DL3/L2 with or without KIR2DS2 (KIR2DL3/L2<sup>high</sup>) or no expression of KIR2DL3, KIR2DL2 and KIR2DS2 (KIR2DL3/L2/S2-) as indicated in Figure 1A(11). CH-L has been reported to bind KIR2DS2, KIR2DL3 and KIR2DL2, whereas REA147 preferentially binds KIR2DL2 and KIR2DL3 compared to KIR2DS2(11). Degranulation (CD107a) was used as a read-out of NK cell activation against malignant B cells in combination with this antibody panel (Figure 1A).

KIR2DS2<sup>high</sup> NK cells had significantly enhanced activation in comparison to both KIR2DL3/L2<sup>high</sup> and KIR2DL3/L2/S2- NK cells against DOHH2 cells (derived from Diffuse Large B cell lymphoma; DLBCL) ( $p < 0.0001$  and  $p < 0.001$  respectively) (Figure 1A,B). We further tested NK cell activation against a panel of B cell lines encompassing mantle cell lymphoma (Mino, Maver-1, Granta-519), Burkitt lymphoma (Ramos, Raji), activated B-cell DLBCL (HBL-1), germinal centre B-cell DLBCL (SU-DHL-6, SU-DHL-4) and ALL (REH) (Figure 1B). These data showed that KIR2DS2<sup>high</sup> NK cells had higher activation than KIR2DL3/L2<sup>high</sup> NK cells against all B cell lines tested, and higher activation than KIR2DL3/L2/S2-negative cells against all cell lines apart from MAVER and Granta-519. To test KIR2DS2<sup>high</sup> NK cell activation against primary tumour cells, we used peripheral blood derived chronic lymphocytic leukaemia (CLL) cells from five different patients as targets. KIR2DS2<sup>high</sup> NK cells had significantly increased activation against CLL cells as compared to other NK cell subgroups; KIR2DL3/L2<sup>high</sup> ( $p < 0.001$ ) and KIR2DL3/L2/S2- ( $p < 0.05$ ) (Figure 1C,D). Together this data demonstrates that KIR2DS2 marks a population of NK cells with enhanced potential for response against malignant B cells.

To test whether this effect was dependent on HLA-C expression by target cells, we used the HLA-null transformed B cell line 721.221 as target cells. In the absence of HLA-C



expression on target cells, both KIR2DS2<sup>high</sup> and KIR2DL3/L2<sup>high</sup> NK cells showed significantly enhanced activation compared to KIR2DL3/L2/S2- NK cells, consistent with the licensing effect of KIR (Figure 1E). However, KIR2DS2<sup>high</sup> cells showed increased activation ( $p < 0.05$ ) compared to KIR2DL3/L2<sup>high</sup> cells in the absence of HLA-C (Figure 1E), indicating that the enhanced activation of KIR2DS2<sup>high</sup> compared to KIR2DL3/L2<sup>high</sup> cells is not solely due a lack of inhibition mediated by KIR2DL3/L2. In accordance with this, KIR2DS2<sup>high</sup> NK cells showed enhanced degranulation in the presence of both high HLA-C expressing (JeKo-1) and low HLA-C expressing (DOHH2) cell lines (Supplementary Figure 1). In addition, KIR2DS2<sup>high</sup> NK cells showed superior activation against targets cells with different HLA-C genotypes (Table 2) compared to KIR2DL3/L2<sup>high</sup> and KIR2DL3/L2/S2- NK cells. These data indicate that KIR2DS2 marks a population of NK cells with enhanced effector function and that this activity is agnostic to HLA-C expression on target cells. Baseline degranulation in the absence of target cells was similar between KIR2DS2<sup>high</sup> cells and KIR2DL3/L2/S2- NK cells and only marginally higher (<2%) than KIR2DL3/L2<sup>high</sup> NK cells (Supplementary Figure 2A). This indicates that basal levels of NK cell activation do not account for this enhanced response.

NK cells promote adaptive immune responses against cancer via production of cytokines(3) and we therefore sought to determine whether KIR2DS2 also marks a population of NK cells with enhanced cytokine production. In response to the DLBCL cell line DOHH2, KIR2DS2<sup>high</sup> NK cells had significantly increased production of IFN $\gamma$  ( $p < 0.01$ ) and TNF $\alpha$  ( $p < 0.01$ ) compared to KIR2DL3/L2<sup>high</sup> NK cells and no difference from KIR2DL3/L2/S2- cells (Figure 2A,B,D,E). To test whether this was a general effect against different target cells, we then assessed NK cell activation against the ALL derived cell line REH. KIR2DS2<sup>high</sup> NK cells had significantly increased production of IFN $\gamma$  compared to KIR2DL3/L2/S2- cells ( $p < 0.01$ ) and significantly increased production of TNF $\alpha$  compared to both KIR2DL3/L2/S2- ( $p = 0.001$ ) and KIR2DL3/L2<sup>high</sup> cells ( $p < 0.05$ ) (Figure 2C,F). Variability in cytokine production between donors was evident as previously reported(43), however KIR2DS2<sup>high</sup> NK cells were significantly associated with increased cytokine production (Figure 2). Although average cytokine production detected was less than 10% for both IFN $\gamma$  and TNF $\alpha$ , this is consistent with previous reports for NK cell activation(44, 45). To further test the association of KIR2DS2 with cytokine expression we used the HLA-C null cell line 721.221 as targets. In accordance with the previous results, KIR2DS2<sup>high</sup> NK cells showed increased IFN $\gamma$  expression against 721.221 cells compared to KIR2DL3/L2<sup>high</sup> and KIR2DL3/L2/S2- NK cells (Supplementary Figure 2B). In the absence of target cells, there was no significant difference in levels of IFN $\gamma$  between the different NK sub-groups, and for TNF $\alpha$  in the absence of target cells KIR2DS2<sup>high</sup> NK cells had significantly lower levels than KIR2DL3/L2/S2- NK cells (Supplementary Figure 2A).

Taken together, these data indicate that KIR2DS2<sup>+</sup> NK cells are primed for activation and to investigate if this effect was specific to malignant B cell targets we tested NK cell activation against cell lines derived from patients with hepatocellular carcinoma. KIR2DS2<sup>high</sup> NK cells showed increased activation in response to SNU-398, HepG2 and PLC/PRF/5 cells compared to KIR2DL3/L2/S2- and KIR2DL3/L2<sup>high</sup> NK cells (Figure 3A-C). This confirms that high KIR2DS2 expression marks a population of NK cells with enhanced potential

for activation against both solid and hematologic cancer cells compared to NK cells with low/absent expression of KIR2DS2.

### **KIR2DS2<sup>high</sup> NK cells have increased CD16 expression and enhanced response to anti-CD20 antibodies**

To define the impact of this enhanced activation on ADCC we investigated CD16 expression on KIR2DS2<sup>high</sup> NK cells by flow cytometry and determined the response of KIR2DS2<sup>high</sup> NK cells to anti-CD20 coated malignant B cells. KIR2DS2<sup>high</sup> NK cells from healthy donors had significantly increased expression of CD16 compared to KIR2DL3/L2<sup>high</sup> and KIR2DL3/L2/S2- NK cells, as measured by both the mean fluorescent intensity (MFI) of the whole subpopulation, and the percentage of CD16-positive NK cells (Figure 4A-C). Importantly, CD56 bright NK cells were excluded from this analysis and therefore differences in CD16 expression were not due to the presence of CD56bright CD16 negative cells within the KIR2DL3/L2/S2- population. We subsequently tested whether increased CD16 expression was associated with enhanced CD16 mediated functional responses. CD56dim NK cell activation was assessed in response to two anti-CD20 antibodies currently in clinical use, rituximab and obinutuzumab. Using healthy human PBMC samples, activation of KIR2DS2<sup>high</sup> NK cells in response to rituximab and obinutuzumab coated DOHH2 lymphoma cells was significantly higher than KIR2DL3/L2<sup>high</sup> and KIR2DL3/L2/S2- NK cells (Figure 4D,E). These results were confirmed using isolated primary human NK cells (Supplementary Figure 2C).

As KIR2DS2<sup>high</sup> NK cells had higher baseline activity than KIR2DL3/L2/S2- cells against DOHH2 cells, we also tested MAVER-1 cells as targets in ADCC assays in which spontaneous KIR2DS2<sup>high</sup> NK cell activity was lower than that of KIR2DL3/L2/S2- cells (see Figure 1B). This allowed assessment of CD16 ligation on NK cell activation in the absence of enhanced natural cytotoxicity in the KIR2DS2<sup>high</sup> population. Consistent with the results for DOHH2 cells, co-incubation of MAVER-1 cells with rituximab and obinutuzumab led to superior activation of KIR2DS2<sup>high</sup> NK cells compared to KIR2DL3/L2<sup>high</sup> NK cells (Figure 4F,G). The addition of rituximab and obinutuzumab also induced activation of KIR2DS2<sup>high</sup> NK cells to a comparable level as KIR2DL3/L2/S2- NK cells, in contrast to the lower activation of KIR2DS2<sup>high</sup> NK cells evident in the absence of CD16 ligation (Figure 4F,G). We then tested whether KIR2DS2 was associated with enhanced ADCC against target cells which lack expression of HLA-C by using the HLA-C null cell line 721.221. In the absence of HLA-C, KIR2DS2<sup>high</sup> NK cells had significantly increased activation against 721.221 cells compared to KIR2DL3/L2<sup>high</sup> and KIR2DL3/L2/S2- NK cells in combination with rituximab (Figure 4H,I). In combination with obinutuzumab, KIR2DS2<sup>high</sup> NK cells showed significantly increased activation against 721.221 cells compared to KIR2DL3/L2/S2- NK cells (Figure 4H,I). Together, these results indicate that KIR2DS2<sup>high</sup> NK cells possess enhanced reactivity to CD16 ligation in response to anti-CD20 antibodies and provide a further functional correlate of KIR2DS2 with beneficial outcomes of cancer.



## **KIR2DS2<sup>high</sup> NK cells express a distinct transcriptional profile associated with enhanced cytotoxicity**

To identify the mechanisms for this enhanced activity, we performed RNA sequencing of healthy human CD3<sup>+</sup> CD56dim NK cells sorted by flow cytometry into three sub-groups; KIR2DS2<sup>high</sup>, KIR2DL3/L2<sup>high</sup> and KIR2DL3/L2/S2<sup>-</sup>. In accordance with the flow cytometry panel used(6), KIR2DL3 was significantly enriched in the KIR2DL3/L2<sup>high</sup> subset compared to KIR2DS2<sup>high</sup> and KIR2DL3/L2/S2<sup>-</sup> cells (Supplementary Figure 3A) (11). Principal Component Analysis indicated that KIR2DS2<sup>high</sup> NK cells had a distinct transcriptional profile compared to KIR2DL3/L2/S2<sup>-</sup> and KIR2DL3/L2<sup>high</sup> NK cells (Figure 5A). Differential expression gene (DEG) analysis showed that KIR2DS2<sup>high</sup> NK cells had 1719 significantly altered genes compared to KIR2DL3/L2<sup>high</sup> cells and 168 significantly altered genes compared to KIR2DL3/L2/S2<sup>-</sup> NK cells (Figure 5B). Specific genes of interest associated with NK anti-tumour responses upregulated in KIR2DS2<sup>high</sup> compared to KIR2DL3/L2/S2<sup>-</sup> NK cells included NKG7, Granzyme B (GZMB) and CCL5 (Figure 5C,D and Supplementary Figure 3A). Furthermore, consistent with our observations by flow cytometry, there was upregulation of the gene FCGR3A which encodes CD16 and a trend ( $p=0.07$ ) for upregulation of FCER1G (the associated Fc $\gamma$  signalling subunit) in KIR2DS2<sup>high</sup> NK cells (Supplementary Figure 3A). Pathway analysis revealed that KIR2DS2<sup>high</sup> NK cells compared to KIR2DL3/L2/S2<sup>-</sup> NK cells have upregulation of pathways including ‘natural killer cell mediated cytotoxicity’ (Supplementary Figure 3B) ( $p<0.005$ ), ‘ribosome’ and ‘oxidative phosphorylation’ (Figure 5E). These changes could be due to licensing of KIR expressing cells, however compared to KIR2DL3/L2<sup>high</sup> cells, KIR2DS2<sup>high</sup> NK cells have upregulation of pathways associated with ‘FCGR activation’, ‘eukaryotic translation elongation’ and ‘eukaryotic translation initiation’ (Figure 5F). Increased ribosome and translational activity is consistent with the enhanced ability of KIR2DS2<sup>high</sup> NK cells to produce cytokines and cytotoxic granules upon recognition of target cells (see Figures 1-3). This data indicates that KIR2DS2<sup>high</sup> NK cells express a unique transcriptional profile, enriched for genes associated with NK cell activation and translation, in accordance with our functional data.

## **Single-cell RNA sequencing confirms that KIR2DS2 is associated with enhanced cytotoxicity**

The high sequence similarity amongst the KIR genes means that many KIR sequencing reads map to multiple genes and are hence discarded by conventional RNA sequencing pipelines, thereby limiting the power of analysis. Our bulk RNA sequencing data was performed on populations of NK cells separated using flow cytometry mediated detection of KIR combinations and hence did not allow discrimination between individual KIR at the single cell level. We therefore developed a novel single-cell RNA sequencing technique (scRNAseq) to sequence full-length KIR based on the RAGE-seq (Repertoire and Gene expression by Sequencing) technique(35) which combines short-read transcriptomic profiling with long-read Nanopore sequencing.

scRNAseq analysis performed on cells from four PBMC donors enriched for NK cells yielded 6525 cells following filtering and quality control, of which 72.2% were NK CD16hi cells and 6.7% were NK CD56 hi (Figure 6A). NK CD16hi Cells were characterised by

the expression of NCR1, CD16 and NKG7 and low levels of CD56, whereas NK CD56hi cells were positive for CD56, NRC1 and negative for CD16 (Supplementary Figure 4A). NK cells were annotated as NK\_CD16hi, NK CD56hi and NK proliferative subgroups using gene expression markers indicated in Figure 6B. No significant differences in the frequency of NK subtypes were found amongst the four donors (Supplementary Figure 4B). The expression of KIR2DS2 and the closely related inhibitory KIR, KIR2DL3, was successfully detected by Nanopore sequencing and mapped to the NK cell populations defined by short-read transcriptomics (Figure 6C). We then assessed the relationship between KIR2DS2 and KIR2DL3 expression with the transcriptomic profile of CD16hi (CD56dim) NK cells. Significantly upregulated genes within the KIR2DS2+ population compared to KIR2DL3/S2- cells included key NK related genes (KLRD1, KIR2DL3, NKG7 and GZMB) (Figure 6D) which were also evident in the bulk RNA sequencing results (see Figure 5 and Supplementary Figure 3A). Gene set enrichment analysis of KIR2DS2+ vs KIR2DS2- CD16hi NK cells revealed that the most significantly upregulated pathway in KIR2DS2+ NK cells was Natural Killer cell mediated cellular cytotoxicity (Figure 6E), confirming our previous functional and bulk RNA sequencing results. NK cells and T cells share common signalling pathways and consistent with an enhanced activation state of KIR2DS2+ NK cells, the T cell receptor signalling pathway was also significantly enhanced. In addition, single cell RNA sequencing allowed us to then compare the transcriptomic profile of KIR2DS2+KIR2DL3- with KIR2DS2+KIR2DL3+ and KIR2DS2-KIR2DL3+ CD16hi NK cells, which was not previously possible due to the high sequence homology between these KIR genes. KIR2DS2+KIR2DL3+ NK cells were more strongly enriched for NK mediated cytotoxicity genes compared to KIR2DS2+KIR2DL3- cells, consistent with NK cell licensing by HLA-C (Figure 6F). Furthermore, KIR2DS2+KIR2DL3- cells showed significantly greater co-expression of KIR3DL1 in comparison to the other NK subgroups (Figure 6G). 50.7% (n=394) of NK cells with long read sequences co-expressed KIR2DS2 and KIR2DL3, with 17.5% (n=136) expressing only KIR2DS2 and 31.8% (n=247) expressing only KIR2DL3 (Figure 6G). KIR2DS2+KIR2DL3- cells showed high levels of expression of *KLRD1* (CD94), *RAC2* (a small GTPase), *GZMH* (granzyme H) and *GZMM* (granzyme M) whereas KIR2DS2+KIR2DL3+ double-positive cells expressed high levels of *PRF1* (perforin), *HCST* (DAP10) and *KLRK1* (NKG2D) (Figure 6H). Together, these data confirm that KIR2DS2+ NK cells possess a transcriptomic profile associated with enhanced cytotoxicity, in accordance with the functional *in vitro* data from this study. This is also in accordance with previous immunogenetic studies demonstrating that KIR2DS2 may be associated with protection against cancer(6).

## Discussion

In this study, we identify that NK cells with high expression of KIR2DS2 have enhanced effector function against malignant cells compared to NK cells with low or absent expression of KIR2DS2. This was demonstrated by both enhanced natural cytotoxicity and ADCC against relevant target cells. Bulk RNA sequencing and a customised single-cell RNA sequencing approach revealed that KIR2DS2+ NK cells are primed for activation, with a distinct transcriptional profile associated with NK cell mediated cytotoxicity and translational activity. Taken together, these results indicate that KIR2DS2-positive NK

cells may potentially represent an attractive cellular entity for the development of future immunotherapeutic strategies.

KIR2DS2-positive donor cells are beneficial for the outcome of cord blood transplantation for haematological malignancies and KIR2DS2 is also associated with reduced incidence in the development of childhood ALL(19, 20). However, studies have not investigated this protection on a mechanistic level. One reason for this may have been the lack of reagents able to discriminate between KIR2DS2 and the closely related inhibitory KIRs KIR2DL3 and KIR2DL2. Previously, KIR2DS2 positive NK cells have been shown to possess enhanced cytotoxic and cytokine activity in response to the AML cell line K562(20) and neuroblastoma cells in vitro and in vivo(21), however, these studies used antibodies unable to differentiate between KIR2DS2 and the inhibitory KIRs KIR2DL2 and KIR2DL3. In this study, using a recently described flow cytometry assay implementing a novel antibody combination, we showed a marked difference in reactivity against cancer targets between KIR2DS2<sup>high</sup> (KIR2DL3/L2<sup>low</sup>) and KIR2DL3/L2<sup>high</sup> NK cells, indicating that cells expressing these different combinations of receptors have discernible differences in function. Recent genetic analysis showed that the presence of KIR2DL2 and/or KIR2DS2 on donor NK cells and the absence of inhibitory KIR2DL1, KIR2DL3 and KIR3DL1 is associated with protection against relapse following stem cell transplant in AML patients(46). However KIR2DL2 and KIR2DS2 are in tight linkage disequilibrium and therefore understanding this protection is not possible using an immunogenetic approach. The results from our study indicate that at the functional level, KIR2DS2 and not KIR2DL2 is associated with enhanced reactivity against cancer cells, and therefore most likely to be the protective factor.

KIR2DS1 directly recognises HLA-C2 on target leukemic cells(47), however no cancer associated ligands for KIR2DS2 have yet been identified. Using a reporter cell line, one study showed that KIR2DS2 can bind cancer cells in a  $\beta$ 2-microglobulin independent manner, however the ligand was not identified and also bound to KIR2DL3(12). Thus this mechanism is unlikely to be relevant to our observations. KIR2DS2 interacts with HLA-C(8, 10, 48) and with HLA-A\*1101(49) however the data presented in this study indicates that KIR2DS2<sup>high</sup> NK cells retain enhanced activation even in the absence of HLA-C on target cells, and thus this gene marks NK cells with general enhanced anti-cancer activity. This indicates that KIR2DS2 may be a promising target for intervention for tumours in which MHC I downregulation contributes to therapy resistance(50). Blocking of HLA-C simultaneously releases inhibitory KIR mediated inhibition and as such could not be used to probe the contribution of this interaction to NK cell activation. However, enhanced activation of KIR2DS2<sup>high</sup> NK cells compared to KIR2DL3/L2<sup>high</sup> cells was observed against targets in the absence of HLA-C, indicating that inhibition by KIR2DL3/L2 was not the driver for the difference between the sub-populations.

RNA sequencing revealed that KIR2DS2+ NK cells have upregulation of pathways including NK mediated cytotoxicity and FCGR signalling, as well as pathways associated with translation, ribosome and oxidative phosphorylation. This supports the functional data and provides a mechanism whereby the enhanced effector functions of KIR2DS2<sup>high</sup> NK cells is evoked. For example, oxidative phosphorylation is required for prolonged NK

activation(51) and translational pathways are key for production of perforin and granzyme B during NK cytotoxic responses(52). Specific genes of interest upregulated included NKG7, which is critical for translocation of CD107a to the cell surface and delivery of cytotoxic molecules to target cells(53), in accordance with the functional data from this study showing enhanced degranulation in the KIR2DS2<sup>high</sup> subset. In addition, the cell death inducing enzyme, granzyme B, was upregulated in KIR2DS2+ NK cells and is released by NK cells to eliminate target cells(54). Interestingly, CCL5 was upregulated in KIR2DS2+ NK cells and this chemokine recruits conventional type 1 dendritic cells into the tumour microenvironment(55, 56). The single-cell RNA sequencing data revealed that KIR2DS2+ NK cells were more cytotoxic when KIR2DL3 was co-expressed. Although we could not assess co-expression of KIR2DL2 in this population due to high gene homology, the functional data indicates that KIR2DS2, but not KIR2DL3 or KIR2DL2 are associated with enhanced NK function. KIR2DL3 and potentially KIR2DL2 are required, at least at a low level, for the education and maximal cytotoxic potential of KIR2DS2+ NK cells. Together, these data indicate that KIR2DS2 marks a population of NK cells which are primed at the transcriptional level for response against target cells. In addition, we provide proof-of-concept that RAGE-seq can be used to assess NK cells and KIR. This technique could be developed in future work to assess the full repertoire of KIR expression by NK cells linked with the transcriptional profile of NK cells. This may prove useful to study KIR not only in cancer but also in infectious diseases and reproductive disorders for which KIR are also strongly associated with outcome(6).

Antibody mediated targeting of tumour cells has revolutionised cancer therapy, with anti-CD20 antibodies such as rituximab in particular defining a new paradigm for the treatment of B cell malignancies(27). The identification that KIR2DS2 marks a population of NK cells with increased CD16 expression and activation in response to anti-CD20 antibodies may therefore allow new approaches to enhance responses. For example, donors with KIR2DS2 may be selected during adoptive NK cell transfer therapies in combination with anti-CD20 antibodies. This data is in accordance with previous studies which identified that KIR2DS2 is associated with enhanced activation in response to tumour targeting antibodies in neuroblastoma and glioblastoma patients(21, 29). Inhibitory KIR/HLA interactions have been shown to inhibit rituximab, but not obinutuzumab induced ADCC(57) and the enhanced rituximab induced ADCC in KIR2DS2<sup>high</sup> compared to KIR2DL3/L2<sup>high</sup> NK populations may therefore be due to reduced inhibitory KIR expression in the KIR2DS2<sup>high</sup> population. In agreement with this, blocking inhibitory KIR with anti-KIR antibodies enhanced cytotoxicity against lymphoma cells in combination with anti-CD20 antibodies(58). In contrast, obinutuzumab induced ADCC is thought to be largely independent from inhibitory KIR/HLA interactions(57), however our findings indicate that obinutuzumab induced activation of NK cells is enhanced in the presence of KIR2DS2. This may not have previously been recognised because of high homology between KIR2DS2 and KIR2DL3/L2 and the difficulties in detection of KIR2DS2 by flow cytometry or conventional RNA sequencing.

Therapeutic targeting of activating KIR has been hampered by the lack of monoclonal antibodies able to discriminate between activating and inhibitory KIR. As such, therapeutic benefit of KIR2DS2 positive NK cells has to date been achieved through selection of

KIR2DS2+ donors during transplantation. Alternatively, therapeutic targeting of KIR2DS2 may be achieved via viral peptide ligands for KIR2DS2(59) or selection of KIR2DS2+ donors in a CAR-NK approach to harness native enhanced NK cell activity(60). In conclusion, our observations indicate that KIR2DS2+ NK cells may be attractive cellular entities for therapeutic strategies against cancer and further pre-clinical studies are now underway to assess this.

## Supplementary Material

Refer to Web version on PubMed Central for supplementary material.

## Acknowledgements

We thank Richard Jewel and Carolann McGuire for technical assistance with flow cytometry. We also thank all patients and volunteers who donated blood used in this study.

## Funding

Funding for this study was provided by a John Goldman Fellowship from Leukaemia UK to M.D.B and grants from the Medical Research Council (519241101) and Cancer Research UK consortium “HUNTER” to S.I.K. The 10X Chromium Controller was funded from a Cancer Research UK Advanced Clinician Scientist Fellowship to Sean Hua Lim (A27179).

## References

1. Chiossone L, Dumas PY, Vienne M, Vivier E. Natural killer cells and other innate lymphoid cells in cancer. *Nat Rev Immunol.* 2018; 18: 671–688. [PubMed: 30209347]
2. Cerwenka A, Lanier LL. Natural killers join the fight against cancer. *Science.* 2018; 359: 1460–1461. [PubMed: 29599226]
3. Bald T, Krummel MF, Smyth MJ, Barry KC. The NK cell-cancer cycle: advances and new challenges in NK cell-based immunotherapies. *Nat Immunol.* 2020.
4. Sabry M, Lowdell MW. Killers at the crossroads: The use of innate immune cells in adoptive cellular therapy of cancer. *Stem Cells Transl Med.* 2020.
5. Hilton HG, Parham P. Missing or altered self: human NK cell receptors that recognize HLA-C. *Immunogenetics.* 2017; 69: 567–579. [PubMed: 28695291]
6. Blunt MD, Khakoo SI. Activating killer cell immunoglobulin-like receptors: Detection, function and therapeutic use. *Int J Immunogenet.* 2020; 47: 1–12. [PubMed: 31755661]
7. Pende D, Falco M, Vitale M, Cantoni C, Vitale C, Munari E, Bertaina A, Moretta F, Del Zotto G, Pietra G, Mingari MC, et al. Killer Ig-Like Receptors (KIRs): Their Role in NK Cell Modulation and Developments Leading to Their Clinical Exploitation. *Front Immunol.* 2019; 10 1179 [PubMed: 31231370]
8. Stewart CA, Laugier-Anfossi F, Vely F, Saulquin X, Riedmuller J, Tisserant A, Gauthier L, Romagne F, Ferracci G, Arosa FA, Moretta A, et al. Recognition of peptide-MHC class I complexes by activating killer immunoglobulin-like receptors. *Proc Natl Acad Sci U S A.* 2005; 102: 13224–13229. [PubMed: 16141329]
9. Yang Y, Bai H, Wu Y, Chen P, Zhou J, Lei J, Ye X, Brown AJ, Zhou X, Shu T, Chen Y, et al. Activating receptor KIR2DS2 bound to HLA-C1 reveals the novel recognition features of activating receptor. *Immunology.* 2021.
10. Naiyer MM, Cassidy SA, Magri A, Cowton V, Chen K, Mansour S, Kranidioti H, Mbirbindi B, Rettman P, Harris S, Fanning LJ, et al. KIR2DS2 recognizes conserved peptides derived from viral helicases in the context of HLA-C. *Sci Immunol.* 2017; 2



11. Blunt MD, Rettman P, Bastidas-Legarda LY, Fulton R, Capizzuto V, Naiyer MM, Traherne JA, Khakoo SI. A novel antibody combination to identify KIR2DS2(high) natural killer cells in KIR2DL3/L2/S2 heterozygous donors. *HLA*. 2019; 93: 32–35. [PubMed: 30381896]
12. Thiruchelvam-Kyle L, Hoelsbrekken SE, Saether PC, Bjornsen EG, Pende D, Fossum S, Daws MR, Dissen E. The Activating Human NK Cell Receptor KIR2DS2 Recognizes a beta2-Microglobulin-Independent Ligand on Cancer Cells. *J Immunol*. 2017; 198: 2556–2567. [PubMed: 28202613]
13. Djaoud Z, Parham P. HLAs, TCRs, and KIRs, a Triumvirate of Human Cell-Mediated Immunity. *Annu Rev Biochem*. 2020; 89: 717–739. [PubMed: 32569519]
14. Bachanova V, Weisdorf DJ, Wang T, Marsh SGE, Trachtenberg E, Haagenson MD, Spellman SR, Ladner M, Guethlein LA, Parham P, Miller JS, et al. Donor KIR B Genotype Improves Progression-Free Survival of Non-Hodgkin Lymphoma Patients Receiving Unrelated Donor Transplantation. *Biol Blood Marrow Transplant*. 2016; 22: 1602–1607. [PubMed: 27220262]
15. Cooley S, Trachtenberg E, Bergemann TL, Saetern K, Klein J, Le CT, Marsh SG, Guethlein LA, Parham P, Miller JS, Weisdorf DJ. Donors with group B KIR haplotypes improve relapse-free survival after unrelated hematopoietic cell transplantation for acute myelogenous leukemia. *Blood*. 2009; 113: 726–732. [PubMed: 18945962]
16. Cooley S, Weisdorf DJ, Guethlein LA, Klein JP, Wang T, Marsh SG, Spellman S, Haagenson MD, Saetern K, Ladner M, Trachtenberg E, et al. Donor killer cell Ig-like receptor B haplotypes, recipient HLA-C1, and HLA-C mismatch enhance the clinical benefit of unrelated transplantation for acute myelogenous leukemia. *J Immunol*. 2014; 192: 4592–4600. [PubMed: 24748496]
17. Weisdorf D, Cooley S, Wang T, Trachtenberg E, Vierra-Green C, Spellman S, Sees JA, Spahn A, Vogel J, Fehniger TA, Woolfrey AE, et al. KIR B donors improve the outcome for AML patients given reduced intensity conditioning and unrelated donor transplantation. *Blood Adv*. 2020; 4: 740–754. [PubMed: 32092137]
18. Hong S, Rybicki L, Zhang A, Thomas D, Kerr CM, Durrani J, Rainey MA, Mian A, Behera TR, Carraway HE, Nazha A, et al. Influence of Killer Immunoglobulin-like Receptors and Somatic Mutations on Transplant Outcomes in Acute Myeloid Leukemia. *Transplant Cell Ther*. 2021.
19. Almalte Z, Samarani S, Iannello A, Debbèche O, Duval M, Infante-Rivard C, Amre DK, Sinnott D, Ahmad A. Novel associations between activating killer-cell immunoglobulin-like receptor genes and childhood leukemia. *Blood*. 2011; 118: 1323–1328. [PubMed: 21613255]
20. Sekine T, Marin D, Cao K, Li L, Mehta P, Shaim H, Sobieski C, Jones R, Oran B, Hosing C, Rondon G, et al. Specific combinations of donor and recipient KIR-HLA genotypes predict for large differences in outcome after cord blood transplantation. *Blood*. 2016; 128: 297–312. [PubMed: 27247137]
21. Gras Navarro A, Kmiecik J, Leiss L, Zekowski M, Engelsen A, Bruserud O, Zimmer J, Enger PO, Chekenya M. NK cells with KIR2DS2 immunogenotype have a functional activation advantage to efficiently kill glioblastoma and prolong animal survival. *J Immunol*. 2014; 193: 6192–6206. [PubMed: 25381437]
22. Cariani E, Pilli M, Zerbini A, Rota C, Olivani A, Zanelli P, Zanetti A, Trenti T, Ferrari C, Missale G. HLA and killer immunoglobulin-like receptor genes as outcome predictors of hepatitis C virus-related hepatocellular carcinoma. *Clin Cancer Res*. 2013; 19: 5465–5473. [PubMed: 23938290]
23. Wisniewski A, Jankowska R, Passowicz-Muszynska E, Wisniewska E, Majorczyk E, Nowak I, Frydecka I, Kusnierczyk P. KIR2DL2/S2 and HLA-C C1C1 genotype is associated with better response to treatment and prolonged survival of patients with non-small cell lung cancer in a Polish Caucasian population. *Hum Immunol*. 2012; 73: 927–931. [PubMed: 22836042]
24. Beksac K, Beksac M, Dalva K, Karaagaoglu E, Tirnaksiz MB. Impact of “Killer Immunoglobulin-Like Receptor /Ligand” Genotypes on Outcome following Surgery among Patients with Colorectal Cancer: Activating KIRs Are Associated with Long-Term Disease Free Survival. *PLoS One*. 2015; 10 e0132526 [PubMed: 26181663]
25. Alomar SY, Alkhouriji A, Trayhyrn P, Alhethel A, Al-Jurayyan A, Mansour L. Association of the genetic diversity of killer cell immunoglobulin-like receptor genes and HLA-C ligand in Saudi women with breast cancer. *Immunogenetics*. 2017; 69: 69–76. [PubMed: 27631728]



26. Seidel UJ, Schlegel P, Lang P. Natural killer cell mediated antibody-dependent cellular cytotoxicity in tumor immunotherapy with therapeutic antibodies. *Front Immunol.* 2013; 4: 76. [PubMed: 23543707]
27. Marshall MJE, Stopforth RJ, Cragg MS. Therapeutic Antibodies: What Have We Learnt from Targeting CD20 and Where Are We Going? *Front Immunol.* 2017; 8 1245 [PubMed: 29046676]
28. Rudnicka D, Oszmiana A, Finch DK, Strickland I, Schofield DJ, Lowe DC, Sleeman MA, Davis DM. Rituximab causes a polarization of B cells that augments its therapeutic function in NK-cell-mediated antibody-dependent cellular cytotoxicity. *Blood.* 2013; 121: 4694–4702. [PubMed: 23613524]
29. Siebert N, Jensen C, Troschke-Meurer S, Zumpe M, Juttner M, Ehlert K, Kietz S, Muller I, Lode HN. Neuroblastoma patients with high-affinity FCGR2A, -3A and stimulatory KIR 2DS2 treated by long-term infusion of anti-GD2 antibody ch14.18/CHO show higher ADCC levels and improved event-free survival. *Oncoimmunology.* 2016; 5 e1235108 [PubMed: 27999754]
30. Bray NL, Pimentel H, Melsted P, Pachter L. Near-optimal probabilistic RNA-seq quantification. *Nat Biotechnol.* 2016; 34: 525–527. [PubMed: 27043002]
31. Pimentel H, Bray NL, Puente S, Melsted P, Pachter L. Differential analysis of RNA-seq incorporating quantification uncertainty. *Nat Methods.* 2017; 14: 687–690. [PubMed: 28581496]
32. Robinson MD, McCarthy DJ, Smyth GK. edgeR: a Bioconductor package for differential expression analysis of digital gene expression data. *Bioinformatics.* 2010; 26: 139–140. [PubMed: 19910308]
33. Ritchie ME, Phipson B, Wu D, Hu Y, Law CW, Shi W, Smyth GK. limma powers differential expression analyses for RNA-sequencing and microarray studies. *Nucleic Acids Res.* 2015; 43: e47. [PubMed: 25605792]
34. Alhamdoosh M, Ng M, Wilson NJ, Sheridan JM, Huynh H, Wilson MJ, Ritchie ME. Combining multiple tools outperforms individual methods in gene set enrichment analyses. *Bioinformatics.* 2017; 33: 414–424. [PubMed: 27694195]
35. Singh M, Al-Eryani G, Carswell S, Ferguson JM, Blackburn J, Barton K, Roden D, Luciani F, Giang Phan T, Junankar S, Jackson K, et al. High-throughput targeted long-read single cell sequencing reveals the clonal and transcriptional landscape of lymphocytes. *Nat Commun.* 2019; 10 3120 [PubMed: 31311926]
36. J. participants in the 1st Human Cell Atlas. Lun ATL, Riesenfeld S, Andrews T, Dao TP, Gomes T, Marioni JC. EmptyDrops: distinguishing cells from empty droplets in droplet-based single-cell RNA sequencing data. *Genome Biol.* 2019; 20: 63. [PubMed: 30902100]
37. Wolf FA, Angerer P, Theis FJ. SCANPY: large-scale single-cell gene expression data analysis. *Genome Biol.* 2018; 19: 15. [PubMed: 29409532]
38. Macosko EZ, Basu A, Satija R, Nemes J, Shekhar K, Goldman M, Tirosh I, Bialas AR, Kamitaki N, Martersteck EM, Trombetta JJ, et al. Highly Parallel Genome-wide Expression Profiling of Individual Cells Using Nanoliter Droplets. *Cell.* 2015; 161: 1202–1214. [PubMed: 26000488]
39. Lebrigand K, Magnone V, Barbry P, Waldmann R. High throughput error corrected Nanopore single cell transcriptome sequencing. *Nat Commun.* 2020; 11 4025 [PubMed: 32788667]
40. Robinson J, Halliwell JA, Hayhurst JD, Flicek P, Parham P, Marsh SG. The IPD and IMGT/HLA database: allele variant databases. *Nucleic Acids Res.* 2015; 43 D423–431 [PubMed: 25414341]
41. Robinson J, Malik A, Parham P, Bodmer JG, Marsh SG. IMGT/HLA database--a sequence database for the human major histocompatibility complex. *Tissue Antigens.* 2000; 55: 280–287. [PubMed: 10777106]
42. Leger, Adrien. a-slide/NanoCount. Zenodo; 2020. January 28, (2020, J. a.-s. N. Z. Adrien Leger
43. Fisher JG, Walker CJ, Doyle AD, Johnson PW, Forconi F, Cragg MS, Landesman Y, Khakoo SI, Blunt MD. Selinexor Enhances NK Cell Activation Against Malignant B Cells via Downregulation of HLA-E. *Front Oncol.* 2021; 11 785635 [PubMed: 34926302]
44. Romee R, Rosario M, Berrien-Elliott MM, Wagner JA, Jewell BA, Schappe T, Leong JW, Abdel-Latif S, Schneider SE, Willey S, Neal CC, et al. Cytokine-induced memory-like natural killer cells exhibit enhanced responses against myeloid leukemia. *Sci Transl Med.* 2016; 8 357ra123

45. Gang M, Marin ND, Wong P, Neal CC, Marsala L, Foster M, Schappe T, Meng W, Tran J, Schaeffler M, Davila M, et al. CAR-modified memory-like NK cells exhibit potent responses to NK-resistant lymphomas. *Blood*. 2020; 136: 2308–2318. [PubMed: 32614951]
46. Guethlein LA, Beyzaie N, Nemat-Gorgani N, Wang T, Ramesh V, Marin WM, Hollenbach JA, Schetelig J, Spellman SR, Marsh SGE, Cooley S, et al. Following Transplantation for Acute Myelogenous Leukemia, Donor KIR Cen B02 Better Protects against Relapse than KIR Cen B01. *J Immunol*. 2021.
47. Pende D, Marcenaro S, Falco M, Martini S, Bernardo ME, Montagna D, Romeo E, Cognet C, Martinetti M, Maccario R, Mingari MC, et al. Anti-leukemia activity of alloreactive NK cells in KIR ligand-mismatched haploidentical HSCT for pediatric patients: evaluation of the functional role of activating KIR and redefinition of inhibitory KIR specificity. *Blood*. 2009; 113: 3119–3129. [PubMed: 18945967]
48. David G, Djaoud Z, Willem C, Legrand N, Rettman P, Gagne K, Cesbron A, Retiere C. Large spectrum of HLA-C recognition by killer Ig-like receptor (KIR)2DL2 and KIR2DL3 and restricted C1 SPECIFICITY of KIR2DS2: dominant impact of KIR2DL2/KIR2DS2 on KIR2D NK cell repertoire formation. *J Immunol*. 2013; 191: 4778–4788. [PubMed: 24078689]
49. Liu J, Xiao Z, Ko HL, Shen M, Ren EC. Activating killer cell immunoglobulin-like receptor 2DS2 binds to HLA-A\*11. *Proc Natl Acad Sci U S A*. 2014; 111: 2662–2667. [PubMed: 24550293]
50. Garrido F, Aptsiauri N, Doorduyn EM, Garcia Lora AM, van Hall T. The urgent need to recover MHC class I in cancers for effective immunotherapy. *Curr Opin Immunol*. 2016; 39: 44–51. [PubMed: 26796069]
51. O'Brien KL, Finlay DK. Immunometabolism and natural killer cell responses. *Nat Rev Immunol*. 2019; 19: 282–290. [PubMed: 30808985]
52. Fehniger TA, Cai SF, Cao X, Bredemeyer AJ, Presti RM, French AR, Ley TJ. Acquisition of murine NK cell cytotoxicity requires the translation of a pre-existing pool of granzyme B and perforin mRNAs. *Immunity*. 2007; 26: 798–811. [PubMed: 17540585]
53. Ng SS, De Labastida Rivera F, Yan J, Corvino D, Das I, Zhang P, Kuns R, Chauhan SB, Hou J, Li XY, Frame TCM, et al. The NK cell granule protein NKG7 regulates cytotoxic granule exocytosis and inflammation. *Nat Immunol*. 2020.
54. Chowdhury D, Lieberman J. Death by a thousand cuts: granzyme pathways of programmed cell death. *Annu Rev Immunol*. 2008; 26: 389–420. [PubMed: 18304003]
55. Bottcher JP, Bonavita E, Chakravarty P, Blees H, Cabeza-Cabrero M, Sammicheli S, Rogers NC, Sahai E, Zelenay S, Reis e Sousa C. NK Cells Stimulate Recruitment of cDC1 into the Tumor Microenvironment Promoting Cancer Immune Control. *Cell*. 2018; 172: 1022–1037. e1014 [PubMed: 29429633]
56. Voshtani R, Song M, Wang H, Li X, Zhang W, Tavallaie MS, Yan W, Sun J, Wei F, Ma X. Progranulin promotes melanoma progression by inhibiting natural killer cell recruitment to the tumor microenvironment. *Cancer Lett*. 2019; 465: 24–35. [PubMed: 31491449]
57. Terszowski G, Klein C, Stern M. KIR/HLA interactions negatively affect rituximab-but not GA101 (obinutuzumab)-induced antibody-dependent cellular cytotoxicity. *J Immunol*. 2014; 192: 5618–5624. [PubMed: 24795454]
58. Kohrt HE, Thielens A, Marabelle A, Sagiv-Barfi I, Sola C, Chanuc F, Fuseri N, Bonnafous C, Czerwinski D, Rajapaksa A, Waller E, et al. Anti-KIR antibody enhancement of anti-lymphoma activity of natural killer cells as monotherapy and in combination with anti-CD20 antibodies. *Blood*. 2014; 123: 678–686. [PubMed: 24326534]
59. Rettman P, Blunt MD, Fulton RJ, Vallejo AF, Bastidas-Legarda LY, Espana-Serrano L, Polak ME, Al-Shamkhani A, Retiere C, Khakoo SI. Peptide: MHC-based DNA vaccination strategy to activate natural killer cells by targeting killer cell immunoglobulin-like receptors. *J Immunother Cancer*. 2021; 9
60. Mehta RS, Rezvani K. Chimeric Antigen Receptor Expressing Natural Killer Cells for the Immunotherapy of Cancer. *Front Immunol*. 2018; 9: 283. [PubMed: 29497427]

### Key points

- KIR2DS2 is associated with high functional activity of NK cells
- KIR2DS2+ NK cells possess a transcriptomic profile associated with cytotoxicity

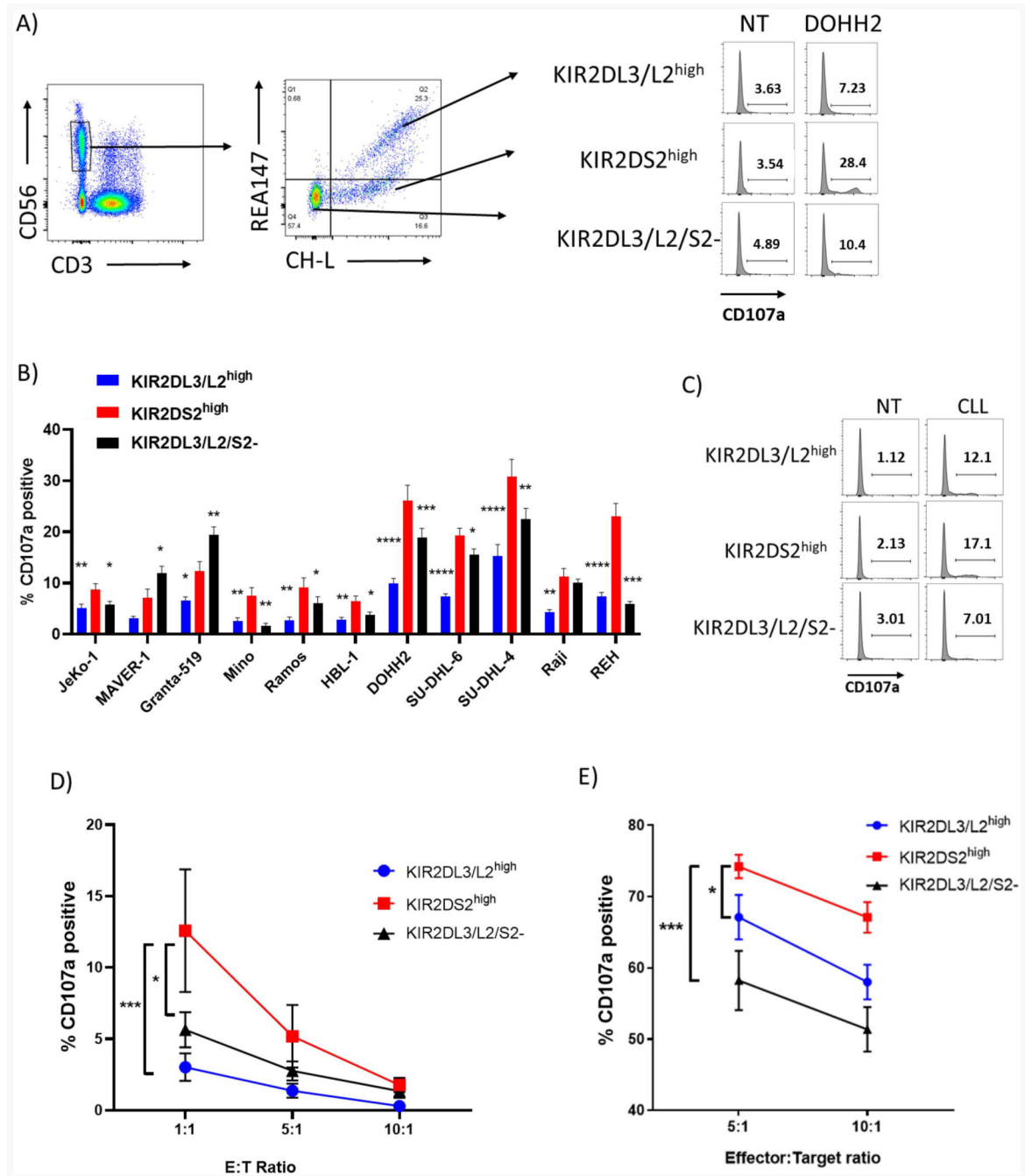


**Figure 1. KIR2DS2<sup>high</sup> NK cells have increased activation against malignant B cells.**

Healthy human PBMC were incubated with IL-15 (1ng/ml) overnight and then co-incubated with DOHH2, REH, Mino, JeKo-1, MAVER-1, Granta-519, Ramos, HBL-1, SU-DHL-6, SU-DHL-4 or Raji (n=10-15) cells or no target (NT) at 5:1 effector:target ratio for 4 hours. CD107a expression was assessed on CD3- CD56dim NK cells separated into KIR2DS2<sup>high</sup>, KIR2DL3/L2<sup>high</sup> or KIR2DL3/L2/S2<sup>-</sup> populations using REA147 and CH-L antibody combinations as shown in A). Representative data against DOHH2 is shown in A) and summarised data as mean  $\pm$  SEM is shown in B) for each indicated cell line. C and

D) Healthy human PBMC from five different donors were incubated with IL-15 (1ng/ml) overnight and then co-incubated with primary human CLL cells from five different donors at 1:1, 5:1 or 10:1 effector:target ratio or no target (NT) for 4 hours. CD107a expression was assessed on CD3- CD56dim NK cells separated into KIR2DS2<sup>high</sup>, KIR2DL3/L2<sup>high</sup> or KIR2DL3/L2/S2- populations. Representative data is shown in C) and summarised data as mean  $\pm$  SEM in D). E) Healthy human PBMC were incubated with IL-15 (1ng/ml) overnight and then co-incubated with 721.221 (n=7) cells at 5:1 and 10:1 E:T ratio for 4 hours. CD107a expression was assessed on CD3- CD56dim NK cells separated into KIR2DS2<sup>high</sup>, KIR2DL3/L2<sup>high</sup> or KIR2DL3/L2/S2- populations. p<0.05 \*, p<0.01 \*\*, p<0.001 \*\*\*, p<0.0001 \*\*\*\*.

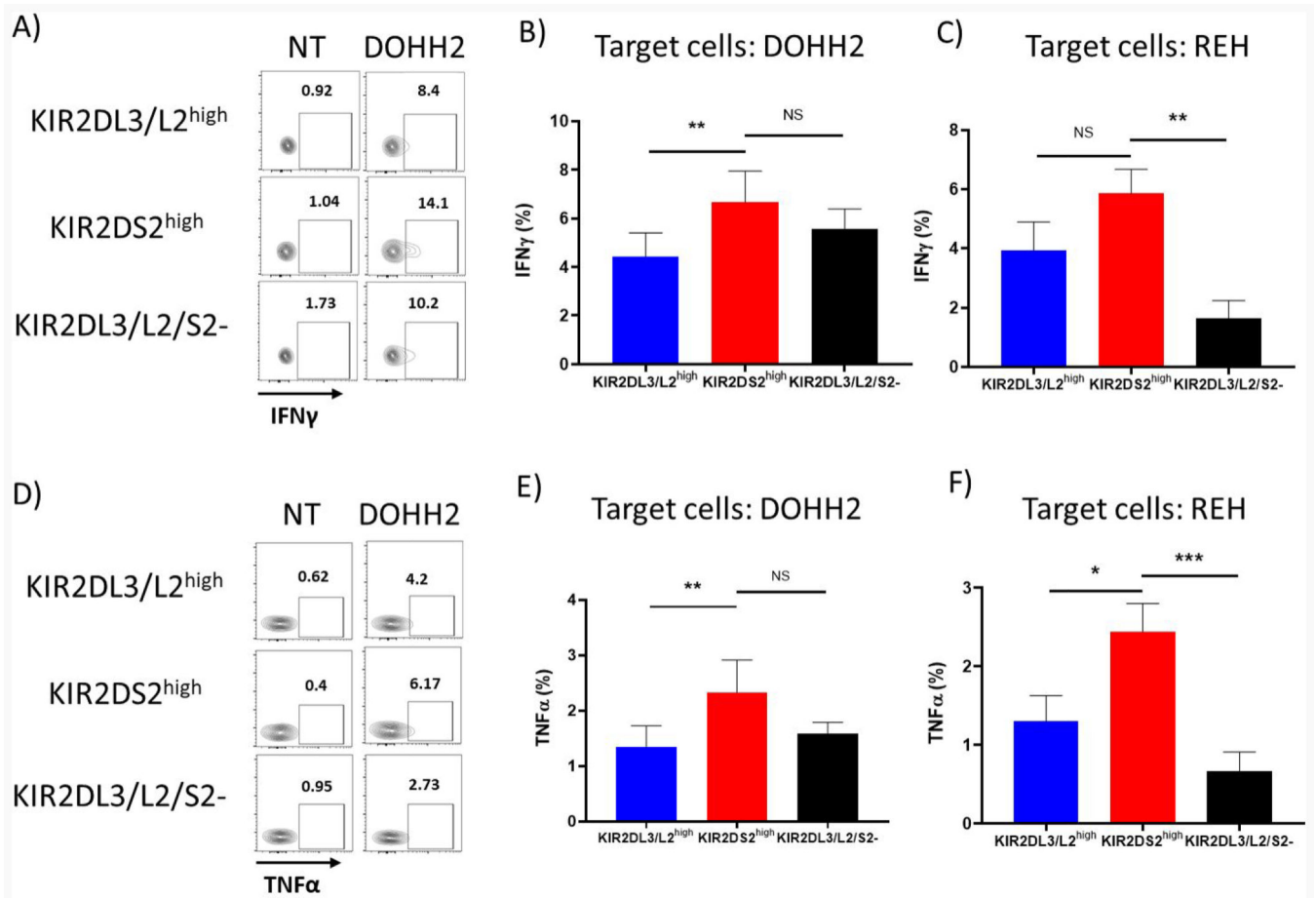


**Figure 2. Enhanced IFN $\gamma$  and TNF $\alpha$  production by KIR2DS2<sup>high</sup> NK cells in response to malignant B cells.**

Healthy human PBMC were incubated with IL-15 (1ng/ml) overnight and then co-incubated with A-B) DOHH2 (n=12) or C) REH (n=8) cells at a 5:1 effector:target ratio or no target (NT) for 4 hours. Cells were then fixed, permeabilized and stained for IFN $\gamma$  and TNF $\alpha$ . Expression was assessed on CD3<sup>-</sup> CD56<sup>dim</sup> NK cells separated into KIR2DS2<sup>high</sup>, KIR2DL3/L2<sup>high</sup> or KIR2DL3/L2/S2<sup>-</sup> populations. Representative flow cytometry plots are shown for IFN $\gamma$  in A) and TNF $\alpha$  in D). Summarised data as mean  $\pm$  SEM for IFN $\gamma$  against DOHH2 cells in B) and REH cells D). Summarised data as mean for TNF $\alpha$  against DOHH2 cells in E) and REH cells F). p<0.05 \*, p<0.01 \*\*, p<0.001 \*\*\*.



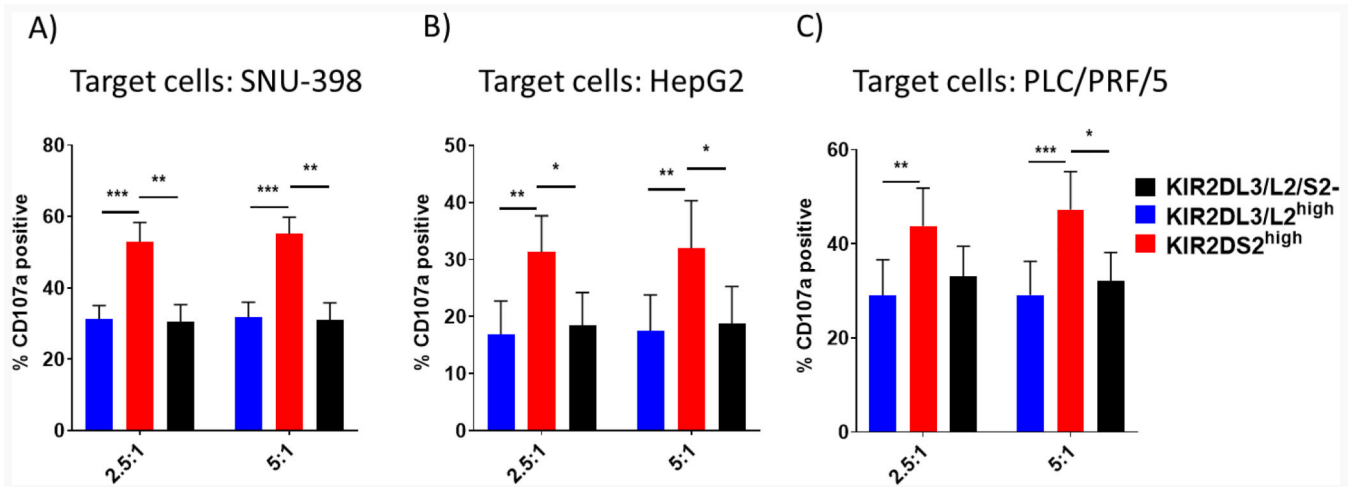


**Figure 3. KIR2DS2<sup>high</sup> NK cells have increased activation against liver cancer derived cell lines.** Healthy human PBMC were incubated with IL-15 (1ng/ml) overnight and then co-cultured with A) SNU-398 (n=7), B) HepG2 (n=9) or C) PLC/PRF/5 (n=9) cells at 2.5:1 or 5:1 effector:target ratios for 4 hours. CD107a expression was assessed on CD3- CD56dim NK cells separated into KIR2DS2<sup>high</sup>, KIR2DL3/L2<sup>high</sup> or KIR2DL3/L2/S2- populations. Data shows mean  $\pm$  SEM CD107a expression on NK cells. p<0.05 \*, p<0.01 \*\*, p<0.001 \*\*\*.

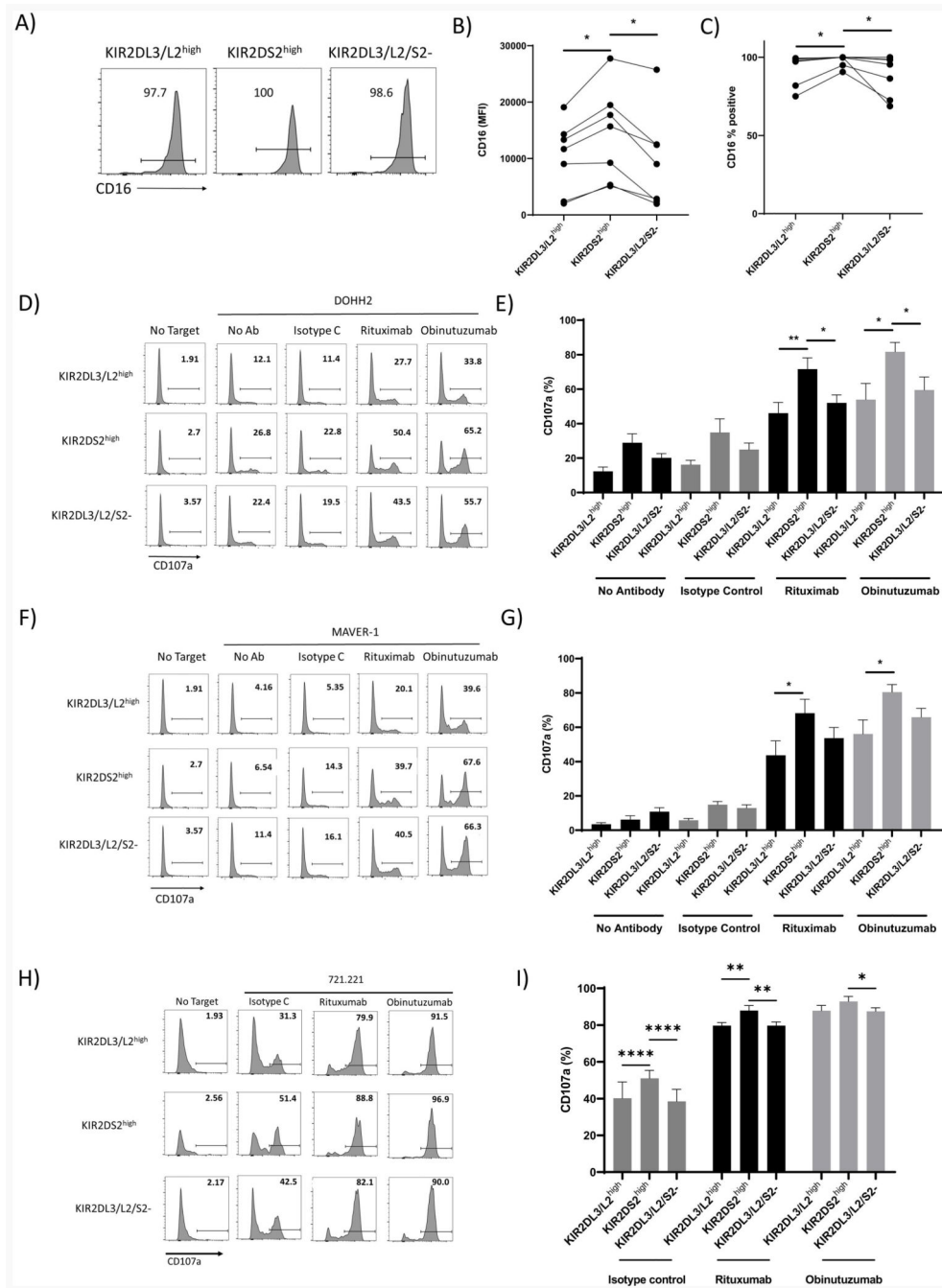


**Figure 4. KIR2DS2<sup>high</sup> NK cells have enhanced CD16 expression and response to anti-CD20 antibodies.**

Expression of CD16 was assessed using flow cytometry on healthy human CD3-CD56dim NK cells. Representative plots are shown in A) and summarised data from seven separate donors is shown in B) as MFI and in C) % positive. D-I) Healthy human PBMC were incubated with IL-15 (1ng/ml) overnight and then co-cultured with DOHH2 (D,E), MAVER-1 (F,G) or 721.221 (H,I) cells at a 10:1 effector:target ratio or no target for 4 hours in the presence of indicated antibodies at 1µg/ml concentration. CD107a expression was assessed on CD3- CD56dim NK cells separated into KIR2DS2<sup>high</sup>, KIR2DL3/L2<sup>high</sup>

or KIR2DL3/L2/S2-populations. Representative plots are shown in D), F) and H) and summarised data shown in E) (n=5), G) (n=5) and in I) (n=7). Data is mean  $\pm$  SEM.  $p < 0.05$  \*,  $p < 0.01$  \*\*,  $p < 0.0001$  \*\*\*\*.

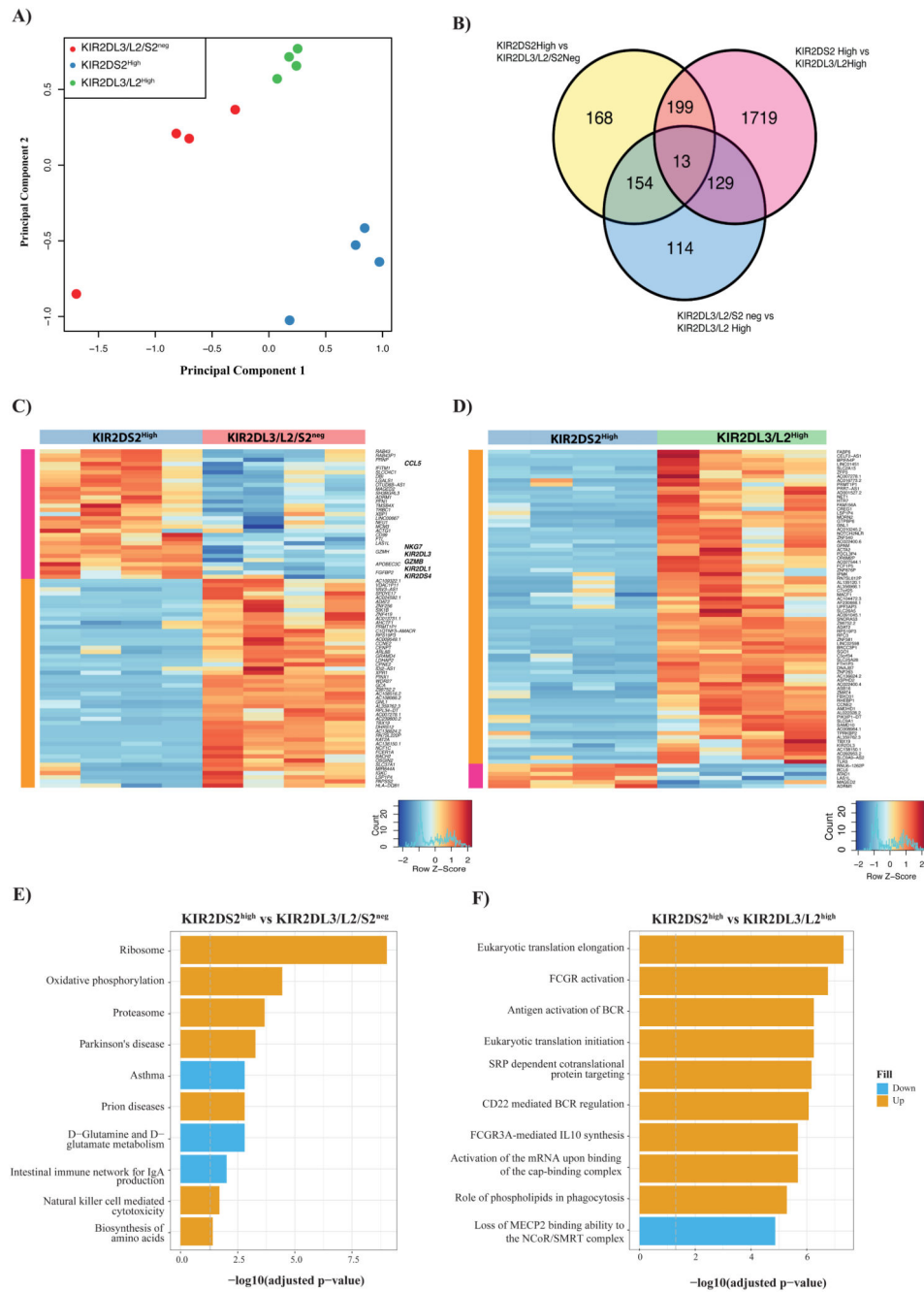


**Figure 5. Bulk RNAseq identifies that KIR2DS2<sup>+</sup> NK cells are primed for activation.** Healthy human CD3<sup>+</sup>-CD56<sup>dim</sup> NK cells were sorted using a BD FACS Aria into KIR2DS2<sup>high</sup>, KIR2DL3/L2<sup>high</sup> or KIR2DL3/L2/S2<sup>-</sup> populations and sequenced using Illumina NovaSeq. A) Principal Component Analysis (PCA) comparison of KIR2DS2<sup>high</sup>, KIR2DL3/L2<sup>high</sup> and KIR2DL3/L2/S2<sup>-</sup> NK cells. B) Venn diagram comparing differential gene expression between KIR2DS2<sup>high</sup>, KIR2DL3/L2<sup>high</sup> and KIR2DL3/L2/S2<sup>-</sup> NK cells. False discovery rate <0.05 from the 3 contrasts analysed. C) and D) Heatmaps showing differential gene expression compared between C) KIR2DS2<sup>high</sup> vs KIR2DL3/L2/S2<sup>-</sup> and

D) KIR2DS2<sup>high</sup> vs KIR2DL3/L2<sup>high</sup>. The top 50 genes of each contrast is shown. Genes were clustered using Pearson correlation and ward.D2 and colour intensity denotes the gene expression level. E) and F) KEGG analysis showing significantly altered pathways between the different subsets of NK cells; E) KIR2DS2<sup>high</sup> vs KIR2DL3/L2/S2- and F) KIR2DS2<sup>high</sup> vs KIR2DL3/L2<sup>high</sup>. The top 10 enriched gene sets are plotted for each contrast. Blue bars show downregulated pathways, whereas orange bars represent upregulated pathways.

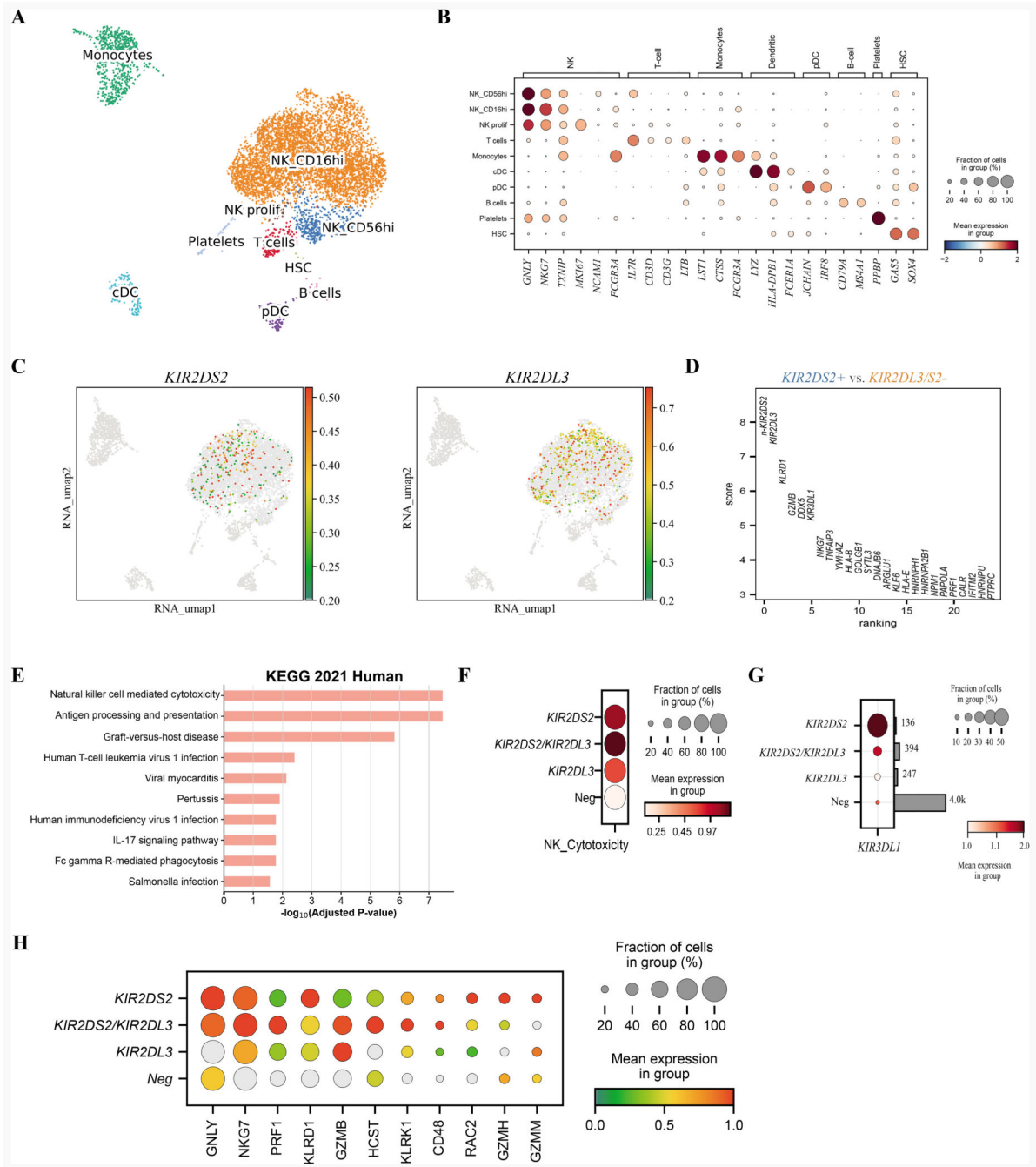


**Figure 6. Single-cell RNA sequencing identifies that KIR2DS2 is significantly associated with NK cell mediated cytotoxicity.**

NK cells from 4 donors were enriched using a negative selection kit. Single cell transcriptome analysis was performed using 3' capture kit (V3.1) from 10X genomics. KIR were pulled down from the full-length cDNA library using specific probes and subsequently sequenced using Nanopore. **A)** Integrated UMAP plot from 4 donors (n= 6525 cells) showing the cluster annotation. **B)** Rank gene analysis showing the marker genes used for cluster annotation. **C)** Detection of KIR2DS2 and KIR2DL3 using long



read sequencing and mapping to the UMAP plot defined by short read transcriptomics. **D)** Differential gene expression comparing KIR2DS2+ vs KIR2DS2- within the CD16hi NK cell population. **E)** Gene set enrichment analysis for the differential expressed genes from the contrast KIR2DS2+ vs KIR2DS2- within the CD16hi NK cell population. Genes used for the analysis had false discovery rates <0.05. KEGG database (2021) was used for the enrichment analysis. The top 10 significant terms are shown. **F)** Gene set enrichment analysis of the NK cytotoxicity gene set (KEGG) among the 4 NK subsets identified using long read sequencing. Colour scales represent mean Z-score. **G)** KIR3DL1 gene expression among the 4 subsets identified using long read sequencing. Colour scales represent mean of gene expression. Side bars shows the number of cells on each category. **H)** Individual gene expression of selected genes from the NK cytotoxicity gene set (KEGG) among 4 NK subsets identified using long read sequencing.

**Table I**  
**Custom probes used for KIR detection**

Gene	Sequence	Scale
KIR2DL3	/5Bios/ CATCCTGCAATGTTGGTCAGATGTCAGGTTTCAGCACTTCCTTCTGCACAGAGAAGGGAAGTTTAAGGACACTTTGCACCTCATTG	4 nmole
KIR2DS2	/5Bios/ GAACAGCGAGGATTCTGATGAACAAGACCATCAGGAGGTGTCATACGCATAATTGGATCACTGTGTTTTACACAGAGAGAAATCA	4 nmole
KIR2D-2	/5Bios/ GCCGCCTGTCTGCACAGACAGCACCATGTCGCTCATGGTCGTCAGCATGGCGTGTGTTGGGTTCTTCTGCTGCAGGGGGCCTGGCCAC	4 nmole
KIR2D-3	/5Bios/ GCCTTACCCACTGAACCAAGCTCCAAAACCGTAACCCAGACACCTGCATGTTCTGATTGGGACCTCAGTGGTCAAATCCCTTCA	4 nmole

**Table II**  
**HLA allele expression of target cell lines**

Cell line	HLA-C allele typing		Reference (PubMed ID)
JeKo-1	C*14:02	C*14:02	25960936
MAVER-1	C*03:03	C*07:02	25960936
Granta-519	C*06:02	C*07:02	25960936
Mino	C*04:01	C*12:03	25960936
REH	C*06:02	C*04:01	26589293
Raji	C*04:01	C*03:04	25960936
SU-DHL-4	C*03:04	C*03:04	26589293
Ramos	C*16:01	C*16:01	25960936
SU-DHL-6	C*07:06	C*03:03	26589293
DOHH2	C*07:04	C*07:04	25960936
HBL-1	NA		NA
SNU-398	C*04:01	C*01:02	26589293
HepG2	C*16:02	C*04:01	25960936
PLC/PRF/5	C*04:01	C*17:01	26589293
721.221	HLA-C null		3257565

NA: Not Available